Available online at www.sciencedirect.com
ScienceDirect
Catalysis Today 136 (2008) 228–234
CATALYSIS TODAY
www.elsevier.com/locate/cattod

Steam reforming of *n*-hexadecane over noble metal-modified Ni-based catalysts

Dae Hyun Kim [a], Jung Shik Kang [a], Yun Joo Lee [a], Nam Kuk Park [c], Young Chul Kim [c], Suk In Hong [b], Dong Ju Moon [a,*]

[a] *Clean Energy Research Center, Korea Institute of Science & Technology, Seoul 130 650, Republic of Korea*
[b] *Department of Chemical & Biological Engineering, Korea University, Seoul, Republic of Korea*
[c] *School of Applied Chemical Engineering, Chonnam University, Gwangju, Republic of Korea*

Available online 13 May 2008

Abstract

Steam reforming of *n*-hexadecane, a main constituent of diesel, over noble metal-modified Ni-based hydrotalcite catalyst was carried out in a temperature range of 700–950 °C, at an atmospheric pressure with space velocity of 10,000–100,000 h^{-1} and feed molar ratio of $H_2O/C = 3.0$. The catalysts were prepared by a co-precipitation and dipping methods. The noble metal-modified Ni-based hydrotalcite catalyst displayed higher resistance for the sintering of active metal than the Ni-based hydrotalcite catalyst prepared by the conventional method. It was found that the Rh-modified Ni-based catalysts showed high resistance to the formation of carbon compared to Ni-based catalysts. The results suggest that Rh-modified Ni-based catalyst can be applied for the steam reforming (SR) reaction of diesel.

Keywords: Steam reforming; *n*-Hexadecane; Ni-based catalyst; Noble metal-modified Ni-based catalyst; Hydrotalcite; Carbon formation

1. Introduction

Hydrogen is the fuel for fuel cell and can be prepared by the reforming of hydrocarbons such as methane, methanol, ethanol, liquefied petroleum gas (LPG), gasoline, kerosene, diesel and other oil derivatives [1,2]. Among the above hydrocarbon fuels, liquid fuels can be used as the energy carriers in many applications, especially, residential power generation (RPG) systems in remote areas and the auxiliary power units (APU) based on solid oxide fuel cell (SOFC) systems. Especially, diesel is an attractive fuel for the production of hydrogen by reforming because of its high gravimetric and volumetric hydrogen density and a well-established delivery infrastructure. The advantages of using liquid hydrocarbons for portable and stationary fuel processors compete some major challenges, as discussed in a recent review [3].

The technologies to reforming of hydrocarbons are steam reforming (SR), partial oxidation (POX) and autothermal reforming (ATR). These three reforming reactions for hexadecane ($C_{16}H_{34}$) as a surrogate of diesel are shown by the following chemical reactions, using an assumption of CO_2 formation for all the carbon involved [4–8]:

$$C_{16}H_{34} + 32H_2O \rightarrow 49H_2 + 16CO_2, \quad \Delta H = 2336\,\text{kJ/mol} \tag{1}$$

$$C_{16}H_{34} + 16O_2 \rightarrow 17H_2 + 16CO_2, \quad \Delta H = -5694\,\text{kJ/mol} \tag{2}$$

$$C_{16}H_{34} + 16H_2O + 8O_2 \rightarrow 33H_2 + 16CO_2, \quad \Delta H = -1739\,\text{kJ/mol} \tag{3}$$

The steam reforming process, which produces high H_2 concentration of around 70% in the crude reformate gas, has widely been used to produce hydrogen from various hydrocarbons. The main products from the steam reforming of hydrocarbons are hydrogen (H_2), carbon monoxide (CO) and carbon dioxide (CO_2), however, the formation of ethane, ethylene and methane is usually observed due to the decomposition of hydrocarbon and methanation reactions.

The main problems associated with the reforming of diesel are related to catalyst degradation during the reaction due to the harsh operating conditions (high temperatures and high H_2O/C

* Corresponding author. Tel.: +82 2 958 5867.
E-mail address: djmoon@kist.re.kr (D.J. Moon).

0920-5861/$ – see front matter © 2008 Elsevier B.V. All rights reserved.
doi:10.1016/j.cattod.2008.01.021

ratios) necessary to obtain high hydrogen yields. The reasons of such degradation include poisoning of the catalysts by sulfur, thermal sintering and extensive carbon formation due to the low H/C ratio and the high molecular weight of the molecules present in diesel fuel. Generally, the compositions of reforming catalyst typically comprise of transition metals (Ni, Co, Fe, etc.) or noble metals (Pt, Pd, Ru, Rh, etc.) deposited or incorporated into carefully engineered supports such as thermally stabilized alumina, doped alumina with promoters to accelerate carbon vaporization [9], mixed metal oxides [10]. In the study for catalysts affording steam reforming of diesel, hydrotalcite precursors are promising candidates. It was reported that the anionic clay-based hydrotalcite-like compounds have been researched [11] as the catalyst of various reactions such as hydrogenation, polymerization and reforming, or the antiacid, antipeptin and stabilizer in the medicinal chemistry. The hydrotalcites or hydrotalcite-like compounds after calcinations have the following properties: high-surface area, basic properties, formation of homogeneous mixtures of oxides with very small crystal size, ''memory effect'', which allows the reconstruction of the original hydrotalcite structure under mild conditions when contacting the product of the thermal treatment with water solutions containing various anions [11]. Takehira and coworkers reported [12–21] that the Ni-loaded catalyst prepared from Mg–Al hydrotalcite-like anionic clay has shown high and stable activity for CO_2 reforming, steam reforming and autothermal reforming of CH_4. Moon et al. reported [22,24] that the Ni-loaded catalyst prepared from Mg–Al hydrotalcite-like anionic clay has shown high and stable activity for steam reforming of LPG. The reforming of diesel over Ni-loaded hydrotalcite-like catalyst has not been reported, yet.

In this work, steam reforming of *n*-hexadecane (*n*-$C_{16}H_{34}$), the main component of diesel, was executed in a fixed bed reactor to evaluate the effect of Rh metal added in Ni-based hydrotalcite-like catalysts for restraining sintering of Ni metal.

2. Experimental

2.1. Catalyst preparation

Nickel nitrate [$Ni(NO_3)_2{\cdot}6H_2O$], aluminum nitrate [$Al(NO_3)_3{\cdot}9H_2O$], magnesium nitrate [$Mg(NO_3)_2{\cdot}6H_2O$] and rhodium(III) chloride ($RhCl_3{\cdot}H_2O$, Rh 38.5–45.55%) with the purity of about 98–99% (Aldrich and Alfa Aesar) were used for the preparation of catalysts without additional purification. The distilled and deionized water was used throughout the whole experiment. The Ni/MgAl oxide catalysts using modified hydrotalcite were prepared by the co-precipitation method reported by Takehira et al. [19] with minor modification. An aqueous solution of the nitrate of Al(III) was added slowly with vigorous stirring into an aqueous solution of sodium carbonate. After disappearing the white powder, an aqueous solution of the nitrates of Mg(II) and Ni(II) was orderly added. The atomic ratio of Ni/Mg was kept at 1.0/2.5. Upon adjusting the pH of this solution to 10 with an aqueous solution of sodium hydroxide, fine greenish slurry was precipitated. The solution was aged at 60 °C for 8 h and then cooled to room temperature. The precipitate was filtered, washed with distilled water until free from hydroxide ion. Then the precipitate was dried at 60 °C for 12 h in air. The Mg(Ni)–Al(O) hydrotalcite-like precursors obtained were calcined in air at 850 °C for 5 h by increasing the temperature at a rate of 5 °C/min to form the precursor of Ni/MgAl.

Rh loading has been done by adopting ''memory effect'' as follows: the powder of Ni/MgAl was dipped in an aqueous solution of Rh(III) chloride, stirred for 2 h at room temperature, dried at 110 °C for 5 h and finally calcined at 850 °C for 5 h to form the precursor of Rh–Ni/MgAl(O) catalysts.

2.2. Characterization of catalysts

The chemical composition of the calcined catalysts was measured by inductively coupled plasma atomic emission spectroscopy (ICP-AES) on a PerkinElmer optima 3300 DV device. Specific surface area of the prepared catalyst was determined by physisorption analyzer (Quantachrome Co., Autosorb-1C). The active metal surface area was measured by chemisorption of CO with a sorption analyzer (Micromeritics Co., Autochem II). Temperature-programmed reduction (TPR) of catalyst was performed using a 5-vol.% H_2/Ar as a reducing gas at a heating rate of 10 °C/min with a sorption analyzer (Micromeritics Co., Autochem II). The X-ray diffraction (XRD) patterns of the catalyst were obtained using Shimazdu XRD-6000 with a Cu Kα radiation at 40 kV and 30 mA.

2.3. Steam reforming of n-hexadecane

Fig. 1 shows the schematic diagram for steam reforming of *n*-hexadecane. The steam reforming of *n*-hexadecane was performed in a fixed bed reactor system. Both preheater (14-mm o.d. and 0.25-m length) and steam reforming reactor (14-mm o.d. and 0.25-m length) were made of an Inconel 6600 tube. The Ni-based catalyst was reduced at 800 °C for 3 h in the hydrogen atmosphere prior to the reaction. The flow rates of *n*-hexadecane and water feeds were controlled by liquid flow controller (LFC) at 7 bar with nitrogen. The feeds were vaporized at 300 °C and preheated at 500 °C before being passed through the catalyst bed in the reactor. The unreacted H_2O was removed by a cold trap and then a gas effluent was analyzed by the on-line gas chromatographs (HP 6890 Series II, TCD and FID) equipped with carbosphere-packed column and DB-2887 capillary column connected to 10-port injector. The qualitative analysis of out gas was measured by GC/MS (HP 5890 Series/MS detector) equipped with HP-1 capillary column. All runs were carried out at a temperature range of 700–950 °C, at an atmospheric pressure with a space velocity of 10,000–100,000 h^{-1} and feed molar ratio of $H_2O/C = 3.0$.

3. Results and discussion

Blank test for the SR of *n*-hexadecane was carried out at 900–950 °C with steam for checking repercussions of thermal cracking of *n*-hexadecane before the catalytic reaction was

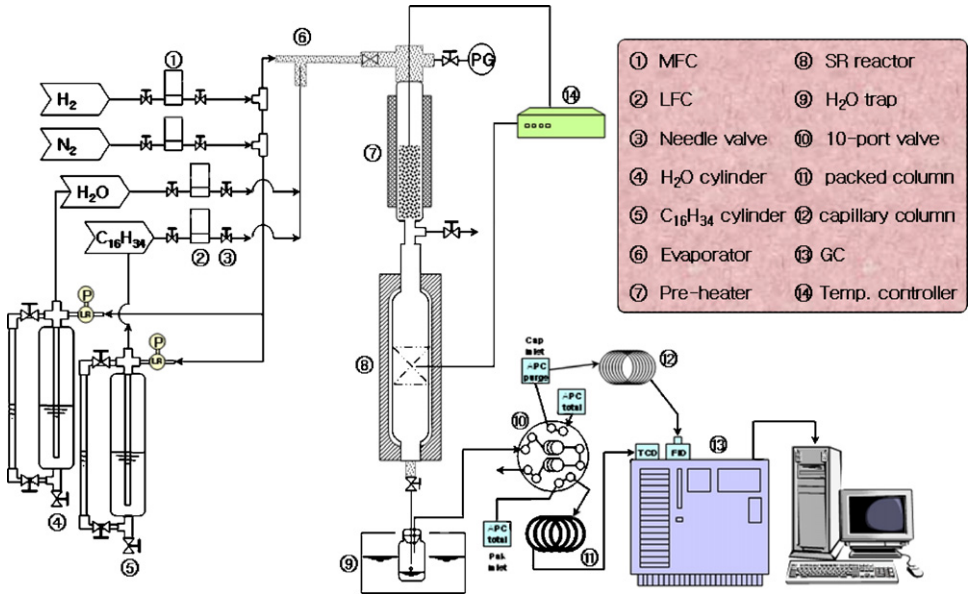

Fig. 1. Schematic diagram for steam reforming of *n*-hexadecane.

started. Under tested conditions, thermal cracking could not maintain over 2 h due to much carbons produced in the reactor. The principal product was CH_4 and a small amount of hydrogen, C_2H_4 was produced. C^{3+} hydrocarbon and *n*-hexadecane obtained in a trace amount.

Depeyre and Flicoteaux reported [25] that most of *n*-hexadecane was almost thermally cracked with steam at 750 °C and C_2H_4, CH_4 and C_3H_6 were formed as major products. A small amount of hydrogen was also produced. They suggested that C_2H_4 and C_3H_6 are mainly responsible for the coke formation during the steam reforming of heavy hydrocarbon which brings about the deactivation of catalyst. In this work,

The catalytic steam reforming of *n*-hexadecane was carried out in the same condition of thermal cracking. This reaction did not produce carbon and C^{2+} hydrocarbon and keep the perfect conversion for *n*-hexadecane during the reaction so the activity of catalyst was evaluated by the reaction product.

The sample designations and their physico-chemical properties are shown in Table 1. Rh-modified Ni/MgAl catalysts were prepared by either the co-precipitation and dipping methods. The nickel contents of all the prepared catalysts were nearly same about 20.0 wt%, as determined by ICP-AES. The BET surface area of Ni/MgAl catalyst after dipping with Rh metal was found to be higher, 100 m^2/g. The dispersion of Rh and Ni metal on Rh-modified Ni/MgAl catalysts were determined by CO pulse chemisorption method. The dispersion was increased with increasing the loading amount of Rh metal. The metal dispersion values allow the quantitative estimation of surface Rh and Ni among the total amount of Rh and Ni loaded. After the SR reaction, active metal dispersion of all catalyst decreased however, spc-Ni/MgAl catalyst without Rh metal diminished drastically.

Fig. 2 shows the XRD patterns of as-synthesized, dried Ni/MgAl hydrotalcite, calcined Ni/MgAl catalyst and Ni/MgAl catalyst after loading with Rh metal followed by calcination. The XRD patterns clearly reveal the formation of Ni/MgAl hydrotalcite in the dried sample (Fig. 2(a)). The reflection line of Ni/MgAl appeared upon after calcination at 850 °C for 5 h (Fig. 2(b)). The hydrotalcite of Ni/MgAl was found to be reconstituted after dipping the calcined sample powders of Ni/MgAl in an aqueous solution of $RhCl_3$ (Fig. 2(c)). After dipping the calcined Ni/MgAl hydrotalcite in the Rh aqueous $RhCl_3$ solution, the reconstitution of hydrotalcite was completed by ''memory effect'' during dipping the solution slowly in water bath. Rh-oxide peak was found to be absent after calcination as observed by Takehira and coworkers [23].

The equilibrium conversion was estimated by PRO/II simulation program <version 8.1>, assuming thermodynamic equilibrium [26]. It was estimated from simulation that the carbon formation did not observed at region of 700–950 °C under the condition of feed molar ratio of $H_2O/C = 3.0$ and GHSV of 10,000 h^{-1}. Also, C^{1+} components such as CH_4,

Table 1
Physico-chemical properties of the catalysts used in this work

Catalyst	Rh loading[a] (wt%)	Ni loading[a] (wt%)	BET[b] (m^2/g)	Total pore volume[b] (cm^3/g)	Average pore diameter[b] (nm)
spc-Ni/MgAl	–	20.0	197.7	0.285	50.7
Rh–Ni/MgAl-A	0.31	20.2	105.4	0.375	101.3
Rh–Ni/MgAl-B	0.52	20.4	107.0	0.316	118.2
Rh–Ni/MgAl-C	1.01	20.1	106.2	0.342	109.4

[a] Determined by ICP-AES.
[b] Measured by Quntachrome Co.

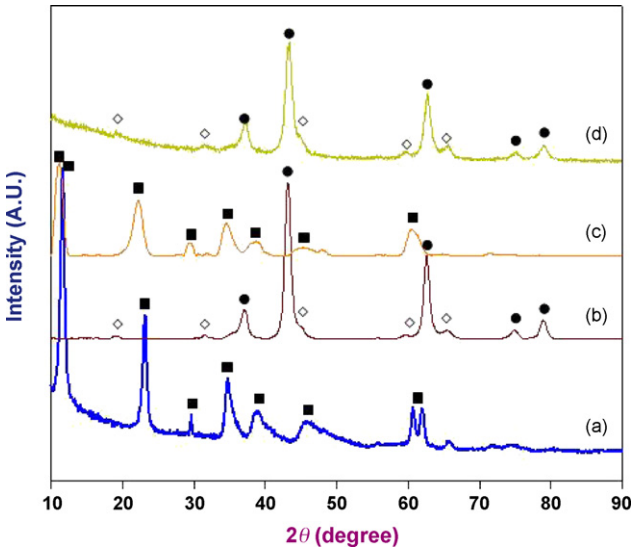

Fig. 2. XRD patterns of prepared catalyst: (a) Ni/MgAl-hydrotalcite; (b) after calcination at 850 °C for 5 h; (c) after dipping (b) in an aqueous solution of Rh(III) chloride and drying; (d) after calcination of 0.3 wt% Rh–Ni/MgAl catalyst; (●) Mg–Ni–O; (◇) Ni–Al_2O_4; (■), hydrotalcite.

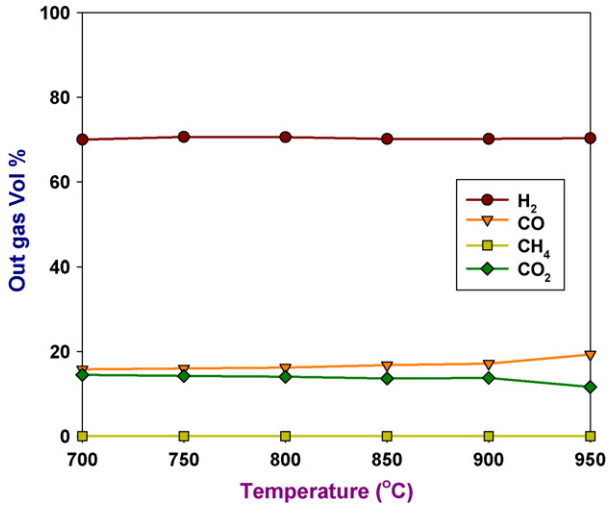

Fig. 3. The out gas volume (%) in steam reforming of *n*-hexadecane over 0.3 wt% Rh–Ni/MgAl catalyst (S/C = 3.0; GHSV = 7000 h^{-1}; temperature = 700–950 °C).

C_2H_4, C_2H_6 and C_3H_6 were not formed in the product stream. The concentration of H_2, CO and CO_2 was about 70%, 16% and 14%, respectively. The SR of *n*-hexadecane over prepared Rh–Ni/MgAl catalysts (Fig. 3) was performed in the temperature range of 700–950 °C, feed molar ratio of H_2O/C = 3 and GHSV of 10,000 h^{-1}. Trends of out gas stream on Rh–Ni/MgAl catalyst resembled each other and it was analogous to the results of calculation by PRO/II simulator except the formation of CH_4 below 750 °C. These results agree well with the theoretical results of SR of heavy hydrocarbon such as *n*-hexadecane.

The SR of *n*-hexadecane on Ni/MgAl and Rh–Ni/MgAl catalyst was carried out at 900 °C, feed molar ratio of H_2O/C = 3 and GHSV of 10,000 h^{-1} for 53 h to confirm the role of Rh metal with restraint of Ni metal sintering (Fig. 4(a) and (b)). The initial activity from start up to 5 h over the spc-Ni/MgAl catalyst was found to be similar to 0.3 wt% Rh–Ni/MgAl catalyst. However, activity of 0.3 wt% Rh–Ni/MgAl was constant during the SR of *n*-hexadecane. On the other hand, activity of Ni/MgAl catalyst slowly decreased with an enhancement in the degree of deactivation from 45 h after the commencement of the reaction. The composition of out gas stream attained the equilibrium state completely after 45 h.

Fig. 5 shows the H_2 and CO concentration of out gas stream for SR of *n*-hexadecane on prepared catalysts in the initial and final reaction at 900 °C and GHSV = 10,000 h^{-1}. The concentration of H_2 after 5 h was nearly same over the prepared catalysts. The reaction was carried out over 0.3 wt% Rh–Ni/MgAl catalyst under the tested condition to corroborate the effect of resistance with Ni metal sintering during the high temperature reaction. The H_2 concentration for the SR over 0.3 wt% Rh–Ni/MgAl catalyst was maintained during the reaction time despite of diminishing the active metal dispersion. However, decrease in H_2 concentration for the

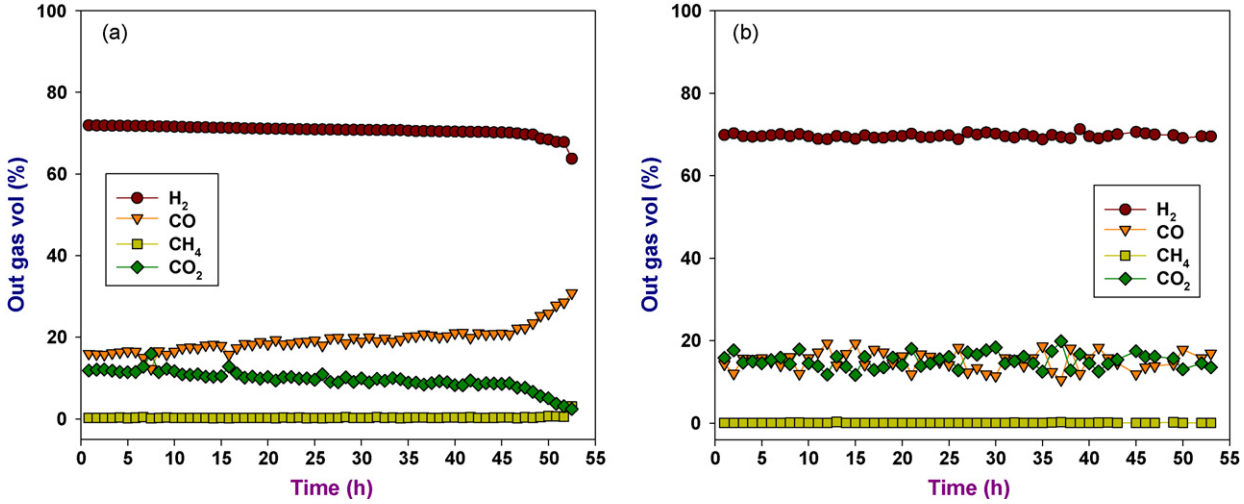

Fig. 4. (a) The out gas volume (%) for SR of *n*-hexadecane on spc-Ni/MgAl catalyst for 53 h (S/C = 3.0; GHSV = 10,000 h^{-1}, Temperature = 900 °C) and (b) The out gas volume (%) for SR of *n*-hexadecane on 0.3 wt% Rh–Ni/MgAl catalyst for 53 h (S/C = 3.0; GHSV = 10,000 h^{-1}; temperature = 900 °C).

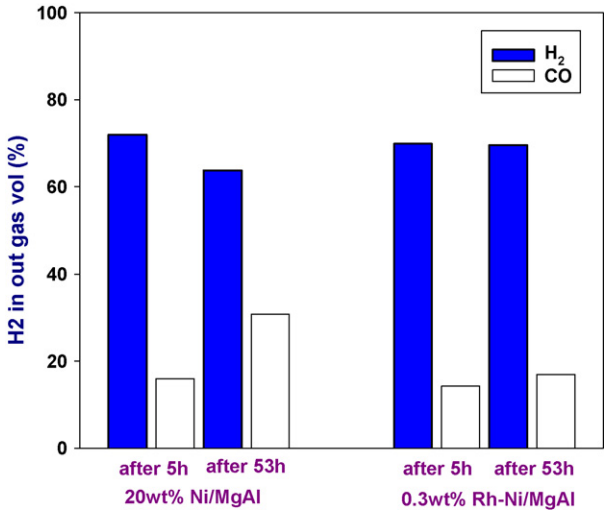

Fig. 5. The H_2 concentration of out gas stream for SR of *n*-hexadecane on prepared catalysts for 53 h (S/C = 3.0; GHSV = 10,000 h^{-1}; temperature = 900 °C).

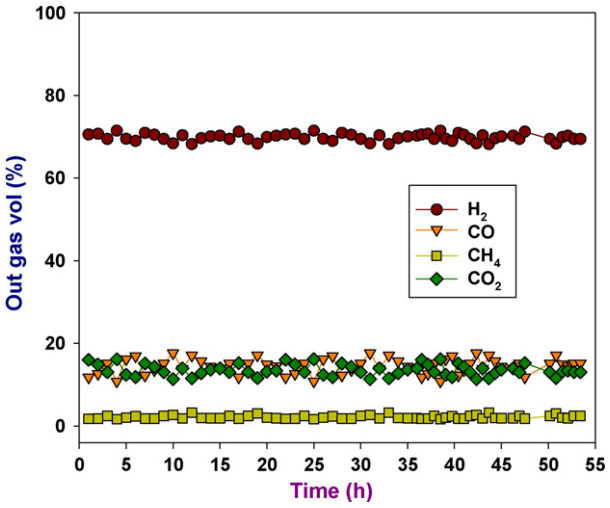

Fig. 6. The out gas volume (%) for SR of *n*-hexadecane on 0.3 wt% Rh–Ni/MgAl catalyst for 53 h (S/C = 3.0; GHSV = 100,000 h^{-1}; temperature = 950 °C).

SR over spc-Ni/MgAl catalyst was due to drastic shrinkage in the metal dispersion and increase in active metal particle size (Table 2). These suggest that the addition of Rh metal to the spc-Ni/MgAl catalyst as promoter was very effective to inhibit the Ni metal sintering for the SR reaction of *n*-hexadecane at high temperature.

Fig. 6 reflects the performance of 0.3 wt% Rh–Ni/MgAl catalyst for SR on *n*-hexadecane at severe conditions such as 950 °C, feed molar ratio of $H_2O/C = 3$ and GHSV of 100,000 h^{-1} for 53 h. The activity of 0.3 wt% Rh–Ni/MgAl catalyst in the SR of *n*-hexadecane under tested conditions was maintained steadily during the reaction time and C^{2+} components such as C_2H_4, C_2H_6 and C_3H_6 were also not formed in the product stream.

Figs. 7 and 8 represent the XRD patterns before and after the reaction of *n*-hexadecane over Ni/MgAl and Rh–Ni/MgAl catalysts at different reaction conditions. The formation of Mg–Ni–O and $NiAl_2O_4$ spinel is due to the repeated heating treatments at 850 °C (Fig. 7(a)). 0.3 wt% Rh was loaded on Rh–Ni/MgAl catalyst. But during dipping process all the Rh was reconstituted, such that Rh-oxide peak was not detected by XRD (Fig. 8(a)). Takehira reported [15] the plausible mechanism of nickel metal crystallization from highly dispersed hydrotalcite-like catalyst prepared by solid phase crystallization method. In the Mg–Al hydrotalcite precursor, a part of Mg sites were substituted by Ni and reconstituted to Ni/MgAl mixed oxide containing Ni^{2+} at the Mg^{2+} site. When the mixed oxide was reduced for the reaction, Ni^{2+} which was reduced to Ni^0 was moved to the surface of the catalyst and crystallized to form fine Ni metal particles. Therefore, spc-Ni/MgAl catalyst has the high activity for SR of light hydrocarbon such as CH_4, methanol and ethanol. However, the reaction condition for steam reforming of heavy hydrocarbon is more severe, high temperature and steam ratio, than that of light hydrocarbon. Fig. 7(b) depicts the XRD patterns of spc-Ni/MgAl catalyst after SR reaction of *n*-hexadecane. The peak intensity of Mg–Ni–O was found to be decreased, while that of $NiAl_2O_4$ strengthened slightly. These signify that the growth of $NiAl_2O_4$ crystallite during the reaction led to diminution of active metal dispersion. Also, reduced Ni metal and graphite carbon peak appeared strongly. These results suggest that the high reaction temperature for steam reforming of *n*-hexadecane accelerated mobility of the reduced Ni metal, ultimately growing up active metal particle by the sintering effect as

Table 2
Characteristics of the catalysts before and after the reaction

Catalyst[a]	BET (m^2/g)[b]		Before the reaction			After the reaction[b]		
	Before	After	Dispersion (%)[c]		Active metal particle size (nm)[c]	Dispersion (%)[c]		Active metal particle size (nm)[c]
			Ni	Ni + Rh		Ni	Ni + Rh	
spc-Ni/MgAl	197.7	42.3	17.12	–	6.33	0.25		401.73
Rh–Ni/MgAl-A	105.4	–	–	12.16	8.34	–	1.04 *	93.23 *
							1.54	66.03
Rh–Ni/MgAl-B	107.0	–	–	13.53	7.50	–	2.75	36.89
Rh–Ni/MgAl-C	106.2	–	–	13.80	7.37	–	3.13	32.41

[a] Catalyst was recovered for the SR of *n*-hexadecane at 950 °C, GHSV = 10,000 h^{-1} (*100,000 h^{-1}) for 53 h^{-1}.
[b] BET surface area was analyzed by measured by Quntachrome Co.
[c] Active metal particle size and dispersion were measured by Micromeritics Co.

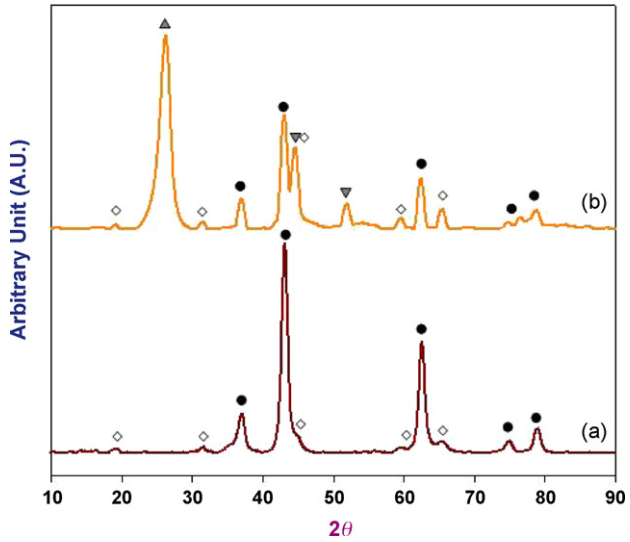

Fig. 7. XRD pattern of prepared catalysts: (a) after calcination of spc-Ni/MgAl; (b) after SR of *n*-hexadecane on Ni/MgAl catalyst at 950 °C, GHSV = 10,000 h^{-1} for 53 h. (●) Mg–Ni–O; (◇) Ni–Al_2O_4; (▼) Ni metal; (▲) carbon.

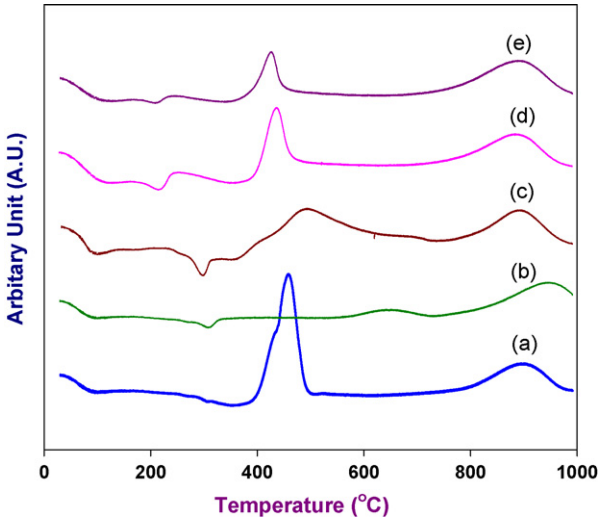

Fig. 9. TPR profile of (a) after dry at 60 °C for 12 h—Ni/MgAl; (b) after calcination at 850 °C—Ni/MgAl; (c) 0.3 wt% Rh–Ni/MgAl after calcinations; (d) 0.5 wt% Rh–Ni/MgAl after calcinations; (e) 1.0 wt% Rh–Ni/MgAl after calcination.

measured by the CO-chemisorption method. On the other hand, when steam reforming of *n*-hexadecane over the 0.3 wt% Rh–Ni/MgAl catalyst was executed at 900 °C for 53 h under GHSV 10,000 h^{-1} and at 950 °C for 53 h under 100,000 h^{-1}, not only the crystal growth of Ni–Al_2O_4 spinel or Mg–Ni–O but also reduction in Ni metal peak intensity was below the detection limit of XRD for used samples. As seen in Fig. 8(b and c), only the intensity of the reflection due to the migrated Rh oxide to the surface of the catalyst form interlayer was found to be slightly increased. These results can infer that the addition of Rh metal promoted the activity of Ni/MgAl catalyst for SR of *n*-hexadecane and restrained the aggregation by moving the reduced Ni metal during the reaction at high temperature.

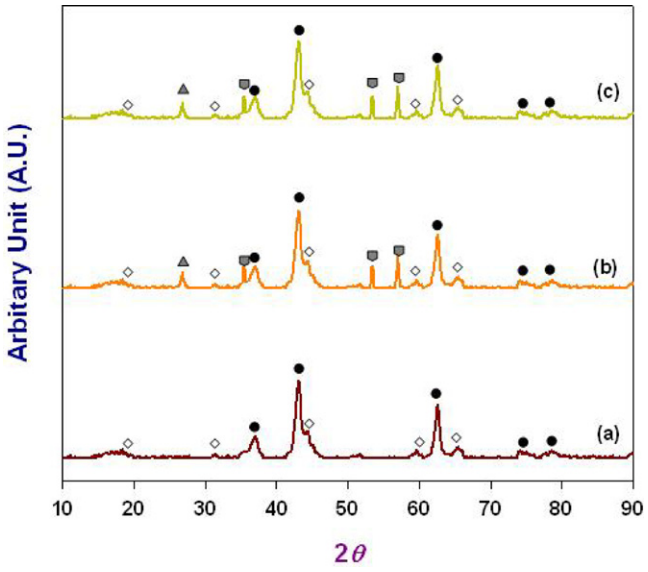

Fig. 8. XRD pattern of prepared catalysts: (a) after calcination of Rh–Ni/MgAl; (b) after SR of *n*-hexadecane at 900 °C, GHSV = 10,000 h^{-1} for 53 h ; (c) after SR of *n*-hexadecane at 950 °C, GHSV = 100,000 h^{-1} for 53 h. (●) Mg–Ni–O; (◇) Ni–Al_2O_4; (⬟), Rh_x–O_x; (▲) carbon.

The TPR profile of prepared catalyst is shown in Fig. 9. The NiO peak in hydrotalcite structure formed after dipping appeared at around 450 °C (Fig. 9(a)) which then disappeared because of the formation of solid Mg–Ni–O solution by calcination (Fig. 9(b)). Rh–Ni/MgAl catalysts displayed two peaks due to the reduction of Rh metal at 230 °C and 425 °C (Fig. 9(c)–(e)). These results reveal that reduction and oxidation of Rh metal is easier than that of Ni metal which agrees with the CO-chemisorption and XRD data. This concludes that Rh metal react with the oxygen source easier than Ni metal due to low reduction temperature and finally suppresses the sintering of Ni metal during the SR of *n*-hexadecane.

4. Conclusions

The spc-Ni/MgAl catalyst derived from a hydrotalcite precursor was prepared by co-precipitation method and Rh–Ni/MgAl catalysts were made by dipping method. Steam reforming of *n*-hexadecane was investigated to figure out the feasibility of modified Ni-based SR catalyst for the RPG and APU applications. The activity of spc-Ni/MgAl catalyst slowly decreased and deactivation accelerated from 45 h. However, 0.3 wt% Rh–Ni/MgAl catalyst maintained the activity during the SR of *n*-hexadecane under the tested conditions. The addition of Rh metal to the spc-Ni/MgAl catalyst as promoter was found to be very effective to inhibit the deactivation of spc-Ni/MgAl catalyst by sintering of reduced Ni metal at high temperature. The results suggest that 0.3 wt% Rh–NiMgAl catalyst was enough to complement the activity of Ni/MgAl catalyst and to control cohering the reduced Ni metal at high temperature.

Acknowledgments

This paper was performed for the development of Hydrogen Station and Fuel Reformer. We would like to thank the KIST for funding this research.

References

[1] L.F. Brown, Int. J. Hydrogen Energy 26 (4) (2001) 381.
[2] D.J. Moon, K. Sreekumar, S.D. Lee, B.G. Lee, H.S. Kim, Appl. Catal. A: Gen. 215 (1–2) (2001) 1.
[3] K. Ahmed, J. Gamman, K. Föger, Solid State Ionics 152/153 (2002) 485.
[4] S. Ayabe, H. Omoto, T. Utaka, R. Kikuchi, K. Sasaki, Y. Teraoka, K. Eguchi, Appl. Catal. A: Gen. 241 (2003) 261.
[5] P.K. Cheekatamarla, A.M. Lane, J. Power Sources 152 (2005) 256.
[6] S. Ahmed, M. Krumpelt, Int. J. Hydrogen Energy 26 (2001) 291.
[7] S.H.D. Lee, D.V. Applegate, S. Ahmed, S.G. Calderone, T.L. Harvey, Int. J. Hydrogen Energy 30 (2005) 829.
[8] A. Qi, S. Wang, G. Fu, D. Wu, Appl. Catal. A: Gen. 293 (2005) 71.
[9] M. Ferrandon, T. Krause, Appl. Catal. A: Gen. 311 (2006) 135.
[10] E. Newson, T.B. Truong, Int. J. Hydrogen Energy 28 (2003) 1379.
[11] F. Cavani, F. Trifirò, A. Vaccari, Catal. Today 11 (1991) 173.
[12] A.I. Tsyganok, K. Suzuki, S. Hamakawa, K. Takehira, T. Hayakawa, Catal. Lett. 77 (2001) 75.
[13] T. Shishido, M. Sukenobu, H. Morioka, R. Furukawa, H. Shirahase, K. Takehira, Catal. Lett. 73 (2001) 21.
[14] T. Shishido, M. Sukenobu, H. Morioka, M. Kondo, Y. Wang, K. Takaki, K. Takehira, Appl. Catal. A: Gen. 223 (2002) 35.
[15] K. Takehira, Catal. Surv. Jpn. 6 (2002) 19.
[16] K. Takehira, T. Shishido, P. Wang, T. Kosaka, K. Takaki, Phys. Chem. Chem. Phys. 5 (2003) 3801.
[17] A.I. Tsyganok, T. Tsunoda, S. Hamakawa, K. Suzuki, K. Takehira, T. Hayakawa, J. Catal. 213 (2003) 191.
[18] K. Takehira, T. Shishido, D. Shoro, K. Murakami, M. Honda, T. Kawabata, K. Takaki, Catal. Commun. 5 (2004) 209.
[19] K. Takihira, T. Shishido, P. Wang, T. Kosaka, K. Takaki, J. Catal. 221 (2004) 43.
[20] K. Takehira, T. Kawabata, T. Shishido, K. Murakami, T. Ohi, D. Shoro, M. Honda, K. Takaki, J. Catal. 231 (2005) 92.
[21] K. Takehira, T. Shishido, D. Shouro, K. Murakami, M. Honda, T. Kawabata, K. Takaki, Appl. Catal. A: Gen. 279 (2005) 41.
[22] D.J. Moon, D.H. Kim, J.S. Kang, J.W. Ryu, B.G. Lee, Y.S. Yoon, B.S. Kwak, Korea Patent 10-2005-00,992 (2005).
[23] T. Miyata, M. Shiraga, D. Li, I. Atake, T. Shishido, Y. Oumi, T. Sano, K. Takehira, Catal. Commun. 8 (2007) 447.
[24] D.J. Moon, D.H. Kim, J.S. Kang, B.G. Lee, S.D. Lee, M.J. Kim, D.H. Sheen, Application Korea Patent (2007).
[25] D. Depeyre, C. Flicoteaux, Ind. Eng. Chem. Res. 30 (6) (1991) 1116.
[26] D.J. Moon, J.W. Ryu, S.D.B.G. Lee, B.S. Ahn, Appl. Catal. A: Gen. 272 (2004) 53.